ZOOLOGICAL SCIENCE **38**: 287–296 (2021)

Heterocypris spadix sp. nov. (Crustacea: Ostracoda: Cypridoidea) from Japan, with Information on Its Reproductive Mode

Mizuho Munakata[1]*, Hayato Tanaka[2], and Keiichi Kakui[3]

[1]*Department of Natural History Sciences, Graduate School of Science, Hokkaido University, Sapporo, Hokkaido 060-0810, Japan*
[2]*Tokyo Sea Life Park, Edogawa-ku, Tokyo 134-8587, Japan*
[3]*Department of Biological Sciences, Faculty of Science, Hokkaido University, Sapporo, Hokkaido 060-0810, Japan*

We describe the cypridoidean ostracod *Heterocypris spadix* sp. nov. from brackish water on Okinawa Island, Japan. The species closely resembles *Heterocypris salina* (Brady, 1868) but differs in that (1) the marginal infolds on valves are less developed, (2) the tubercles on the anterior margin of the right valve are completely covered by the selvage and invisible in inner view, and (3) the calcified inner lamella on the ventral margin of the left and right valves is scarcely evident in inner view, as the ventral margins of the valves bend inwardly. We determined partial sequences for the cytochrome *c* oxidase subunit I (COI; cox1) and 18S rRNA genes in *H. spadix* for future DNA barcoding and phylogenetic analyses. Our sample contained only females. A breeding experiment revealed that *H. spadix* females reproduce parthenogenetically. Another experiment showed that *H. spadix* has low tolerance to desiccation, with all individuals at 25°C dying between 1–2 hours after removal from water. We amplified and sequenced a partial 16S rRNA sequence for the endosymbiotic bacterium *Cardinium* from *H. spadix*. Infection by *Cardinium* may be related to the parthenogenetic reproductive mode we observed in *H. spadix*.

Key words: Brackish, *Cardinium*, endosymbiotic bacteria, mangrove, parthenogenesis, Podocopa, Podocopida, reproduction manipulating, seed shrimp

INTRODUCTION

Species in the cypridoidean genus *Heterocypris* Claus, 1892 characteristically have tubercles on the right-valve margin, have the larger left valve overlapping the smaller right valve around the entire free margin, and lack a dorsal hump on the left valve (Meisch, 2000). To date, about 70 species have been described worldwide (Martens et al., 2019; Meisch et al., 2019; Savatenalinton, 2020; Smith and Chang, 2020) from various non-marine aquatic environments, including freshwater ponds, rice fields, temporary puddles, river mouths, and brackish ponds (Karanovic, 2012). *Heterocypris* shows two reproductive modes: bisexual reproduction and parthenogenesis (Meisch, 2000). Some species contain bisexual as well as parthenogenetic lineages (mixed reproduction), e.g., *Heterocypris barbara* (Gauthier and Brehm, 1928) (Rossi et al., 2007). Infections with *Cardinium*, a group of "reproduction-manipulating" endosymbiotic bacteria, has been reported in several parthenogenetic *Heterocypris* lineages (e.g., Schön et al., 2018; Schön and Martens, 2019).

To date, four *Heterocypris* species have been reported from Japan: *Heterocypris auricularis* Zhai and Zhao, 2014; *H. barbara*; *Heterocypris incongruens* (Ramdohr, 1808); and *Heterocypris savatenalintonae* Smith and Chang, 2020 (Okubo, 1972, 1973, 1975, 2004; Broodbakker, 1988; Okubo and Ida, 1989; Okubo and Terauchi, 1992; Hiruta and Smith, 2001; Smith and Kamiya, 2006; Smith et al., 2011; Tanaka et al., 2015; Smith and Chang, 2020). In addition, Okubo (2004) and Tabuki and Hashimoto (2012) reported unidentified *Heterocypris* individuals. All previous reports were from freshwater environments, mostly temporary water bodies such as rice fields (Fig. 1A).

During a survey on Okinawa Island, Japan, we collected a species of *Heterocypris* from a brackish stream along a mangrove forest. It closely resembles *Heterocypris salina* (Brady, 1868) but can be distinguished from the latter by valve morphology. Here we describe this species as new, report the results of experiments to determine its reproductive mode and desiccation tolerance, present nucleotide sequences for parts of the mitochondrial cytochrome *c* oxidase subunit I (COI) and nuclear 18S rRNA (18S) genes, and show with a molecular marker (16S rRNA; 16S) that this species is infected by *Cardinium*.

MATERIALS AND METHODS

Collection and maintenance of ostracods

Mud sediment including ostracods was collected from a brackish stream along a mangrove forest near the Manko Waterbird &

* Corresponding author. E-mail: munakata.mizuho.k0@elms.hokudai.ac.jp
doi:10.2108/zs200127
http://zoobank.org/5ED8A0FA-7D00-44A9-9856-05B92329EC64

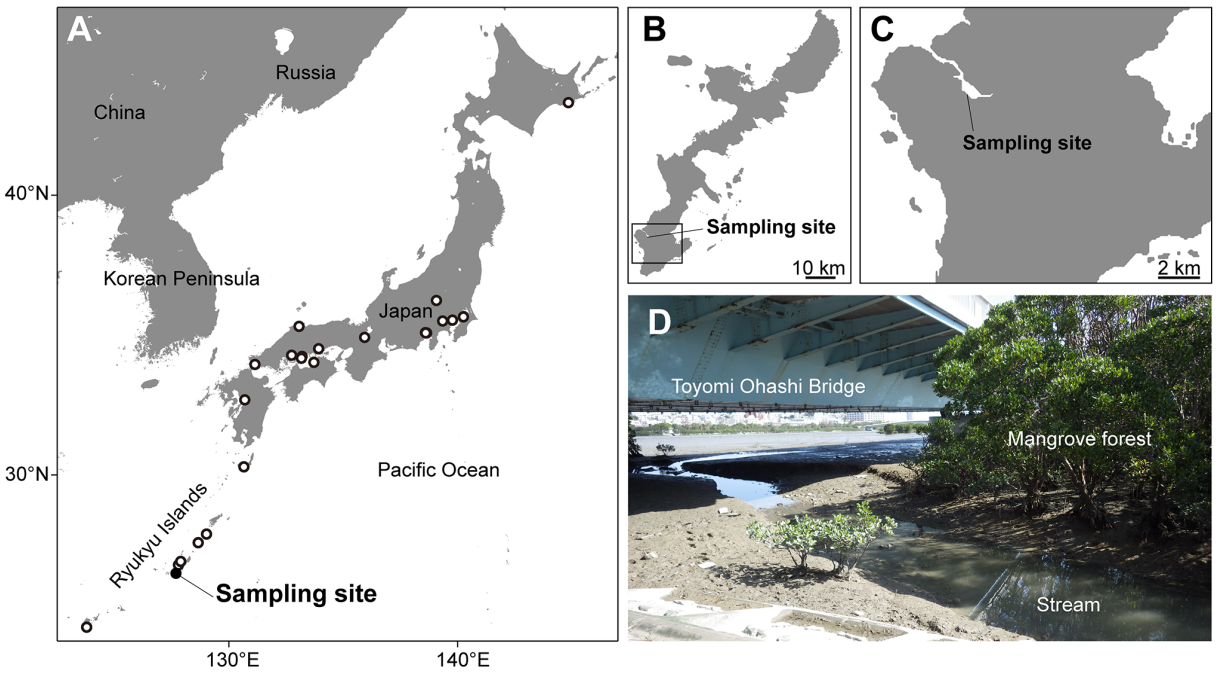

Fig. 1. Sampling site of *Heterocypris spadix* sp. nov. **(A)** map showing the sampling site on Okinawa and previously reported sites for *Heterocypris* individuals in Japan; one site in Broodbakker (1988), presumed to be a typographical error, is not included. **(B)** location of sampling site in Okinawa Island; a square in **(B)** indicates the position of enlargement in **(C)**. **(C)** location of sampling site in southern area of Okinawa Island. **(D)** photograph of the sampling site at the lowest tide.

Wetland Center on Okinawa Island, Okinawa, Japan (26°11′40.6″N 127°40′55.3″E) on 21 November 2018 (Fig. 1). The sediment sample was placed in water in a small aquarium, and the ostracods were maintained for several months (25°C; 14 h L/10 h D; salinity 7‰), and fed every three days with porphyrized dry feed for crayfish (JAN code 4971618829092; Kyorin, Japan). Individuals hatched in the aquarium were used in this study.

Morphology

Ostracods were fixed in 80% ethanol; one individual was photographed before fixation to document its pigmentation pattern. Soft parts were separated from the valves, dissected with sharpened needles under an Olympus SZX9 stereomicroscope, and mounted on glass slides in the mounting agent Neo-Shigaral (Shiga Konchu Fukyusha, Japan). The valves (all bearing complete inner margins) were brushed gently in a 1:3 mixture of commercial bleach (Kitchen Haiter, Kao, Japan) and deionized water (DW) to remove soft tissues and the membranous inner lamellae, washed several times in DW, air dried, and preserved on cardboard slides. The valves and soft parts were observed under an Olympus BX51 light microscope and drawn by using a camera lucida. The fine structure of the dried valves was observed and photographed under the BX51 microscope. Four ethanol-fixed, air-dried ostracods and four pairs of opened valves were prepared for examination by scanning electron microscope (SEM). They were attached to aluminum stubs with carbon double-sided tape (Cat. ID 7321, Nisshin EM, Japan), coated with gold in a Hitachi E-1045 ion sputter coater, and observed at 15 kV accelerating voltage with a Hitachi S-3000N SEM. All material studied has been deposited in the Invertebrate Collection of the Hokkaido University Museum (ICHUM), Sapporo, under catalog numbers ICHUM-6128 to 6145, and 6162 to 6164.

We used the following abbreviations in the text: LV, left valve; RV, right valve; H, height; L, length; W, width; AMI, maximum length of the marginal infold (Yamada and Keyser, 2010) on the anterior valve margins; PMI, maximum length of the marginal infold on the posterior valve margins; An1, antennula; An2, antenna; Md, mandible; Mx, maxillula; L5–7, fifth, sixth, and seventh limbs, respectively; UR, uropodal ramus. The appendages chaetotaxy follows Broodbakker and Danielopol (1982) for An1, Md, and Mx; Martens (1987) for An2; Meisch (2000) for L5–7; and Meisch (2007) for UR.

The following measurements were made from digital images by using ImageJ (Rasband, 2020): L, H, AMI, and PMI of the LV and RV (LV-L, LV-H, LV-AMI, LV-PMI, RV-L, RV-H, RV-AMI, and RV-PMI); W of the carapace (Ca-W); length ratio from the second to seventh podomeres of An1; L and W of the second palpal podomere of the Mx; length ratio from the third to sixth podomeres and terminal claw (h2) of L6; L of the UR ramus (UR-L); W at the narrowest portion of the UR ramus (UR-W); and length ratio of claws G_a, G_p and setae S_a and S_p on the UR. Measurements in the description are presented as the range followed by the mean and sample size in parentheses. Measurements of carapaces and appendages in congeners were obtained from descriptions or, when not given, were measured from illustrations.

Breeding experiments

To determine the reproductive mode of the population we investigated, six female ostracods from the aquarium were isolated (parental generation: P), each in one well of a six-well cell culture plate (25°C; 14 h L/10 h D; 7‰ salinity; fed every three days), and checked for spawning and hatching every 1–3 days under the SZX9 stereomicroscope. Maternal individuals were retained in the wells until their juveniles had been isolated. Within three days after hatching, we isolated one to three juveniles (F_1 generation, all females) from each maternal individual and reared them singly under the same conditions as described above. Two juveniles (F_2 generation, both females) from one F_1 mother were isolated within 24 hours after hatching and maintained until spawning.

Desiccation experiment

To evaluate desiccation tolerance, we carried out the following

experiment. Fifty-two adults that had not been fed for 2 days were isolated in brackish water (salinity 7‰), each in one well of twelve-well cell-culture plates. As much of the water as possible was removed from each well with a Pasteur pipette, after which the plates were maintained at 25°C ("drying treatment"; humidity was not recorded). At 1, 2, 4, 6, and 8 hours at 25°C (here termed the 1 h-, 2 h-, 4 h-, 6 h-, and 8 h-drying treatment), 12, 10, 10, 10, and 10 wells, respectively, were refilled with brackish water (7‰). To complete the experiment, the individuals surviving in each treatment were counted 1 hour and 1 day after rehydration.

DNA analysis

An individual (ICHUM-6135) that had not been fed for one day to remove its gut contents was fixed in 80% ethanol, and its soft parts were detached from the carapace. Total DNA was extracted from the soft parts by using a NucleoSpin Tissue XS Kit (TaKaRa Bio, Japan) following the manufacturer's protocol. Primers used for PCR and sequencing are listed in Table 1. PCR amplification conditions for COI with TaKaRa Ex Taq DNA polymerase (TaKaRa Bio) were 94°C for 1 min; 35 cycles of 98°C for 10 s, 50°C for 30 s, and 72°C for 50 s; and 72°C for 2 min. Conditions for 18S amplification with KOD FX Neo (Toyobo Life Science, Japan) were 94°C for 1 min; 45 cycles of 98°C for 10 s, 65°C for 30 s, and 72°C for 50 s; and 72°C for 2 min. All nucleotide sequences were determined by direct sequencing with a BigDye Terminator Kit ver. 3.1 with a 3730 DNA Analyzer (Life Technologies, USA). Fragments were concatenated by using MEGA7 (Kumar et al., 2016).

The COI sequence we determined (658 nt, encoding 219 amino acids) was aligned by using CLUSTAL W (Thompson et al., 1994) with all *Heterocypris* COI sequences currently deposited in the International Nucleotide Sequence Database (INSD): *H. incongruens* from Turkey (accession number KF991575; Kubanç et al., 2017), *H. salina* from Egypt (three sequences, LC319787, LC324690, LC324691; Ali et al., 2018), and *Heterocypris* sp. from Italy (MH916762; Schön et al., 2018). The aligned sequences were trimmed with MEGA7 to the shortest length among them (489 nt). Kimura (1980) 2-parameter (K2P) distances among the aligned sequences were calculated with MEGA7.

PCR amplification and direct DNA sequencing of the 16S sequence from *Cardinium* were carried out with the primers listed in Table 1. PCR amplification conditions with TaKaRa Ex Taq DNA polymerase were 94°C for 1 min; 35 cycles of 98°C for 10 s, 50°C for 30 s, and 72°C for 1 min; and 72°C for 2 min. Fragments were concatenated by using MEGA7.

The sequences we determined were deposited in the INSD through the DNA Data Bank of Japan, under accession numbers LC557032 (ostracod COI), LC557033 (ostracod 18S), and LC589665 (*Cardinium* 16S).

Table 1. List of PCR and cycle sequencing (CS) primers used in this study.

Gene	Primer	Sequence	Reaction	Source
COI	LCO1490	GGTCAACAAATCATAAAGATATTGG	PCR & CS	Folmer et al. (1994)
	HCO2198	TAAACTTCAGGGTGACCAAAAAATCA	PCR & CS	Folmer et al. (1994)
18S	SR1	TACCTGGTTGATCCTGCCAG	PCR	Nakayama et al. (1996)
	SR8	GGATTGACAGATTGAGAGCT	CS	Nakayama et al. (1996)
	SR9	AACTAAGAACGGCCATGCAC	CS	Nakayama et al. (1996)
	SR12	CCTTCCGCAGGTTCACCTAC	PCR & CS	Nakayama et al. (1996)
	EU929R	TTGGCAAATGCTTTCGC	CS	Puitika et al. (2007)
	18S554f	AAGTCTGGTGCCAGCAGCGCG	CS	Maraun et al. (2009)
	18S614r	TCCAACTACGAGCTTTTTAACC	CS	Maraun et al. (2009)
16S	ChF	TACTGTAAGAATAAGCACCGGC	PCR & CS	Zchori-Fein and Perlman (2004)
	ChR	GTGGATCACTTAACGCTTTCG	CS	Zchori-Fein and Perlman (2004)
	CLO-f1	GGAACCTTACCTGGGCTAGAATGTATT	CS	Gotoh et al. (2007)
	CLO-r1	GCCACTGTCTTCAAGCTCTACCAAC	PCR & CS	Gotoh et al. (2007)

RESULTS

Taxonomy

Family **Cyprididae** Baird, 1845
Genus ***Heterocypris*** Claus, 1892
Heterocypris spadix sp. nov.
(Figs. 2–6)

Etymology. The specific name *spadix* is a Latin adjective meaning chestnut-colored, referring to the carapace color of this species.

New Japanese name. *Yakime-ibo-kaimijinko*, referring to the pale-yellow-colored carapace with a mottled dark-brown pattern that resembles scorch marks. The Japanese noun *yakime* means "scorch marks"; *Ibo-kaimijinko* is the Japanese name for *Heterocypris*.

Material examined. Holotype: Female, ICHUM-6128, two slides. Paratypes (20 females): ICHUM-6129, undissected, one vial; ICHUM-6130, 6131, one SEM stub and one slide for each; ICHUM-6132–6134, 6162–6164, one SEM stub for each; ICHUM-6135, two slides, voucher specimen for LC557032 (COI) and LC557033 (18S); ICHUM-6136–6145, one slide for each. All specimens were hatched in an aquarium and were the descendants of individuals collected from the type locality, a brackish stream along a mangrove forest near the Manko Waterbird & Wetland Center on Okinawa Island, Okinawa, Japan (26°11′40.6″N 127°40′55.3″E) (see Materials and Methods).

Description of females. Measurements (in millimeters, except for ratios) of carapace and valves: LV-L 1.07–1.17 (1.12, *n* = 10), LV-H 0.66–0.72 (0.69, *n* = 10), LV-H/LV-L 0.60–0.63 (0.62, *n* = 10); RV-L 1.06–1.15 (1.10, *n* = 10), RV-H 0.63–0.69 (0.66, *n* = 10), RV-H/RV-L 0.58–0.62 (0.60, *n* = 10); Ca-W 0.40–0.48 (0.44, *n* = 9), Ca-W/LV-L 0.44–0.54 (0.49, *n* = 9); LV-AMI 0.114–0.122 (0.118, *n* = 10); LV-PMI 0.051–0.069 (0.057, *n* = 10); RV-AMI 0.095–0.103 (0.099, *n* = 10); RV-PMI 0.037–0.044 (0.041, *n* = 10).

Carapace (Figs. 2–4, 5A, B) pale yellowish in color, mottled with dark-brown (Fig. 2A–C; faded in ethanol); outer surface smooth but with sparse tiny setae; fine granular background and overlying reticulation (cf. Smith and Chang, 2020) present (Fig. 3F); widest point behind mid-length of carapace (Fig. 3B); subanterior right margin weakly depressed in dorsal view (Fig. 3B); posterior end rounded in dorsal view (Fig. 3B).

LV slightly overlapping RV along entire margin, with slight dorsal expansion (Fig. 3A–D); greatest height at about mid-length

Fig. 2. *Heterocypris spadix* sp. nov., female, paratype (ICHUM-6129), fresh specimen. **(A–C)** left, right, and dorsal views, respectively. Scale bar: 0.5 mm.

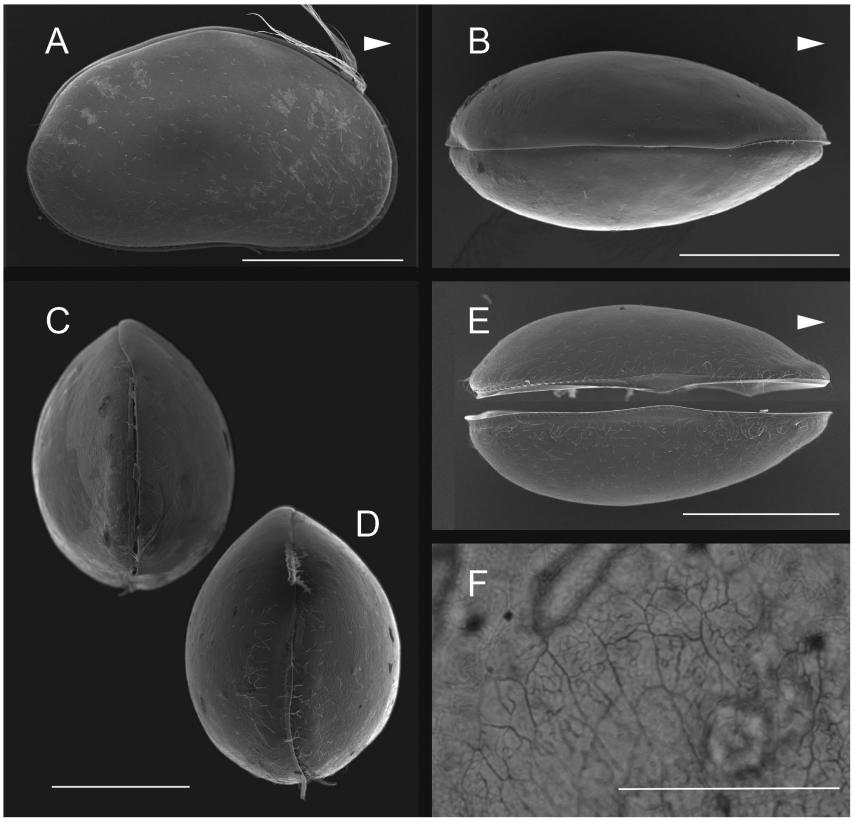

Fig. 3. SEM and light microscope images of carapaces and valves of female *Heterocypris spadix* sp. nov. **(A)** paratype (ICHUM-6162). **(B)** paratype (ICHUM-6134). **(C)** paratype (ICHUM-6132). **(D)** paratype (ICHUM-6133). **(E)** paratype (ICHUM-6163). **(F)** paratype (ICHUM-6128). **(A–D)** right, dorsal, anterior, and posterior views of whole carapace. **(E)** ventral view of LV and RV. **(F)** light microscope image of reticulated pattern on RV. Arrowheads indicate anterior. Scale bars: **(A, B, E)** 0.5 mm, **(C, D)** 0.3 mm, **(F)** 0.1 mm.

of LV; anterodorsal margin smooth, slightly convex; posterodorsal margin with weak cardinal angle; anterior and posterior margins evenly rounded (posterior slightly more sharply than anterior); ventral margin slightly concave; apex of anterior margin lower than mid-height of LV and slightly higher than apex of posterior margin; in inner view, inner list present in anterior region (Fig. 4C), posterior flange present (Fig. 4C); marginal infold on anterior and posterior margins not well developed (Figs. 4C, 5A); calcified inner lamella on ventral margin almost invisible in inner view as ventral margin bends inward (Figs. 4C, 5A).

RV similar to LV, but lacking dorsal expansion; outer list present in ventral region (Fig. 3E); anteroventral selvage reaching outer edge of valve, completely covering tiny tubercles on anteroventral margin (Fig. 4D, d1, E); posteroventral selvage not reaching outer edge of valve, with tubercles on posterovental margin exposed (Fig. 4D, d2, F). Two oblong mandibular muscle scars and five oblong adductor muscle scars on LV and RV (Fig. 4C, D). Hinge adont. Dark brown eye near base of An1 (Fig. 2A–C).

An1 (Fig. 5C) with seven podomeres. Podomere length ratio from second to seventh podomeres 17 : 27 : 18 : 13 : 10 : 13. First podomere with one dorsal and two ventrodistal plumed setae; Wouters organ button-shaped. Second podomere with dorsodistal plumed seta reaching middle of third podomere; Rome organ button-shaped. Third podomere with dorsodistal seta reaching tip of sixth podomere and ventrodistal seta reaching middle of fourth podomere. Fourth podomere with two dorsodistal setae as long as podomeres 2–7 and two ventrodistal setae reaching middle of sixth podomere. Fifth podomere with two long dorsodistral setae (one as long as podomeres 1–7; one as long as podomeres 2–7) and two shorter ventrodistal setae. Sixth podomere with four outer distal setae as long as podomeres 1–7 and shorter inner distal seta. Seventh podomere with three distal setae (two long, subequal; one short, ca. half the length of long ones) and aesthetasc y_a (ca. 40% length of long setae).

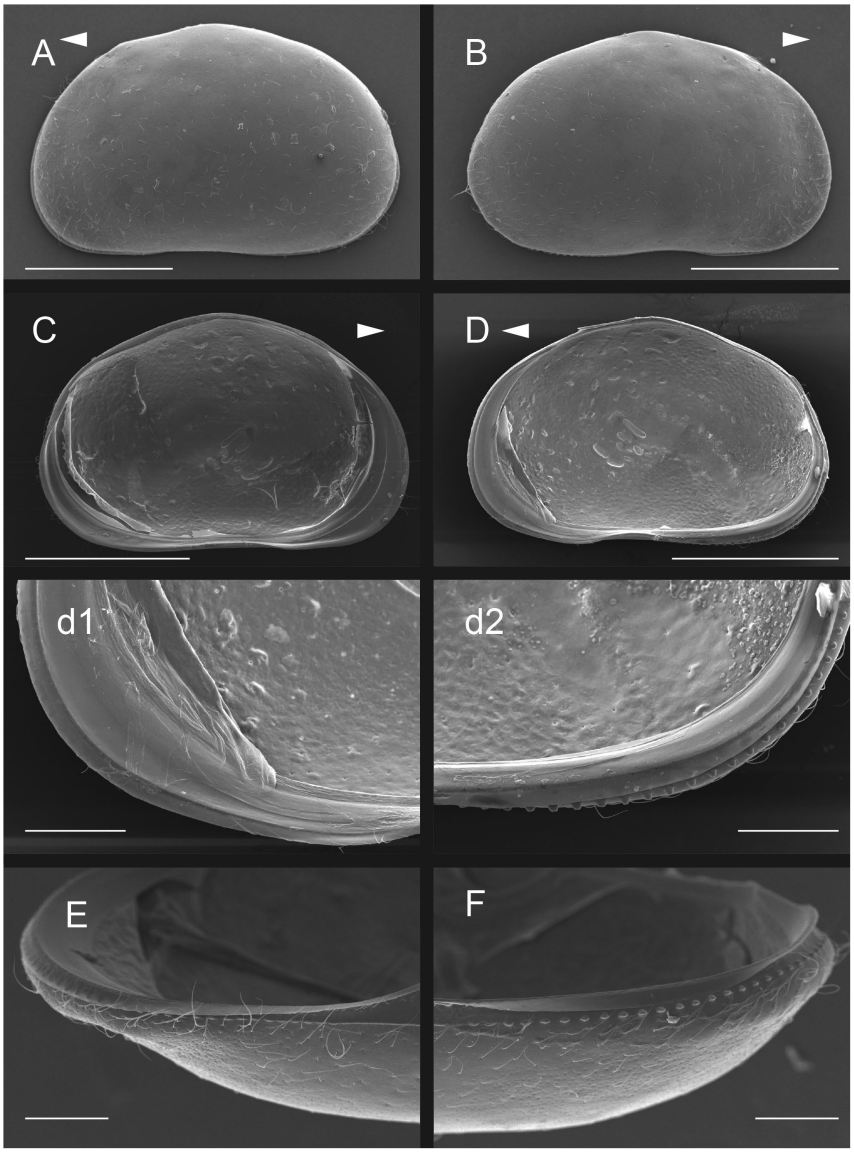

Fig. 4. SEM images of valves of female *Heterocypris spadix* sp. nov. **(A, B)** paratype (ICHUM-6131). **(C, D)** paratype (ICHUM-6130). **(E, F)** paratype (ICHUM-6164). **(A, B)** LV and RV, outer views. **(C, D)** LV and RV, inner views. **(d1, d2)** anterior and posterior areas of RV, inner views. **(E, F)** anterior and posterior areas of RV, inner ventral views. Arrowheads indicate anterior. Scale bars: **(A–D)** 0.5 mm, **(d1, d2, E, F)** 0.1 mm.

An2 (Fig. 5D, E) with five podomeres. First podomere (coxa) with three ventral plumed setae. Second podomere (basis) with ventrosubdistal seta extending beyond tip of third podomere. Exopodite with one long and two unequal short setae. Third (first endopodal) podomere with six inner subdistal natatory setae extending beyond tips of claws $G_{1-3,M}$, ventrodistal plumed seta reaching tip of fifth podomere, and mid-ventral aesthetasc Y. Fourth podomere undivided, with two mid-dorsal setae, dorsosubdistal setae z_{1-3} of unequal length, mid-ventral plumed setae t_{1-4} reaching middle of claws $G_{1,3}$, mid-ventral short aesthetasc y_1, ventrodistal short aesthetasc y_2 (Fig. 5E), and distal claws G_{1-3} (Fig. 5E); claw G_2 ca. 80% length of claws $G_{1,3}$. Fifth podomere (Fig. 5E) with plumed seta g reaching to ca. 75% of claw G_M, bifurcate aesthetasc y_3 (longer part half the length of claw G_M), and claws $G_{m,M}$; G_m ca. 60% length of G_M; G_M reaching tip of claws $G_{1,3}$.

Md (Fig. 5F, f1) with coxa, palp comprising four podomeres (one basal and three endopodal), and vibratory plate. Coxa with 10 distal teeth and three subdistal plumed setae. First podomere (basis) with one ventrodistal seta, ventrodistal setae $S_{1,2}$, and ventrodistal seta α (ca. half the length of setae $S_{1,2}$); setae $S_{1,2}$ subequal in length, bearing row of long setules. Vibratory plate (exopodite) with four rays. Second (first endopodal) podomere with three dorsodistal setae of unequal length (longest reaching tip of claws on fourth podomere), five mid-ventral long plumed setae (not extending beyond tip of claws on fourth podomere), and mid-ventral plumed short seta ß (shorter than half the length of mid-ventral plumed setae). Third podomere with four dorsosubdistal setae and two ventrosubdistal setae; inner region with distal plumed seta γ and three distal plumed setae (Fig. 5f1). Fourth podomere with distal seta and four distal claws.

Mx (Fig. 6A, a1) with palp comprising two podomeres, three endites, and vibratory plate. First palpal podomere with seven dorsodistal setae of unequal length (two of them plumed). Second palpal podomere not spatula-like, but rectangular, L/W ca. 2, with three distal setae and three distal claws. First endite with two ventroproximal plumed setae and 10 distal setae. Second endite with nine distal setae. Third endite with two distal serrated spines (Fig. 6a1) and seven distal setae (two of them plumed). Vibratory plate with 14 rays.

L5 (Fig. 6B) with protopod, palp, and vibratory plate. Protopod with two setae a, plumed seta b, plumed seta d, and 13 distal plumed setae of unequal length. Palp with distal plumed setae h_{1-3}. Vibratory plate with four rays.

L6 (Fig. 6C) with six podomeres (border between first and second podomeres indistinct). Length ratio from third to sixth podomeres and terminal claw (h2) 60 : 35 : 29 : 10 : 87. First and second podomeres (protopod) with seta d_1 but without seta d_2. Third (first endopodal) podomere with ventrodistal plumed seta e reaching middle of fifth podomere. Fourth podomere not fused to fifth podomere; with ventrodistal plumed seta f not reaching tip of fifth podomere. Fifth podomere with very short ventrodistal seta and ventrodistal plumed seta g. Sixth podomere with dorsodistal plumed seta h_3, ventrodistal plumed seta h_1, and distal curved claw h_2.

L7 (Fig. 6D) with four podomeres, bearing pincer organ

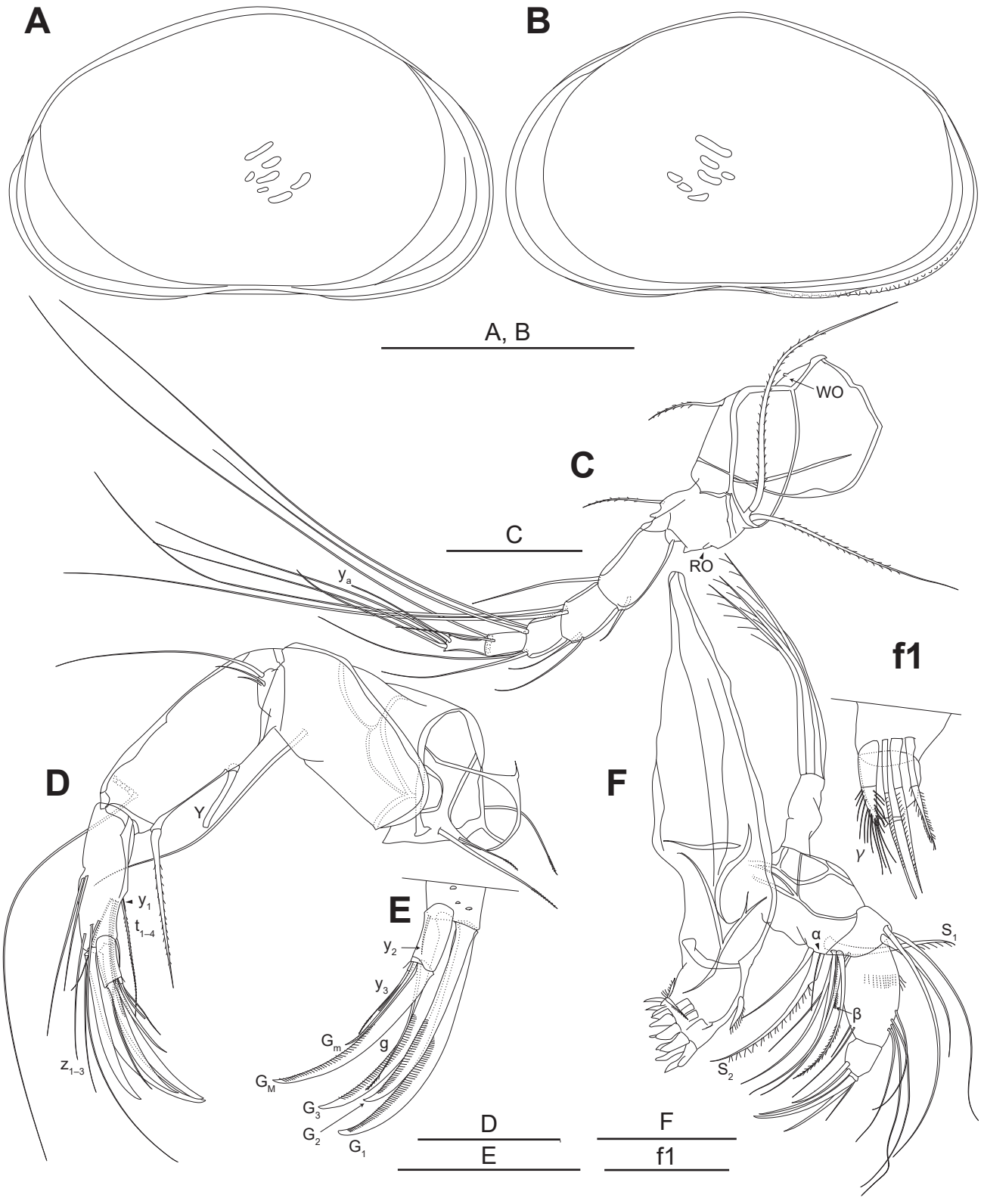

Fig. 5. *Heterocypris spadix* sp. nov., female. **(A–D, F)** holotype (ICHUM-6128). **(E)** paratype (ICHUM-6130). **(A, B)** LV and RV, inner views (tiny marginal setae omitted). **(C)** An1 (three of four long setae on sixth podomere omitted). **(D)** An2, outer view (five of six natatory setae on third podomere omitted). **(E)** distal area of An2, outer view (setae Z_{1-3} omitted). **(F)** Md, outer view (setules on four of five mid-ventral setae on second podomere and four inner plumed setae on third podomere omitted). **(f1)** third and fourth podomeres of Md, inner view. Scale bars: **(A, B)** 0.5 mm, **(C–F)** 0.1 mm, **(f1)** 0.05 mm.

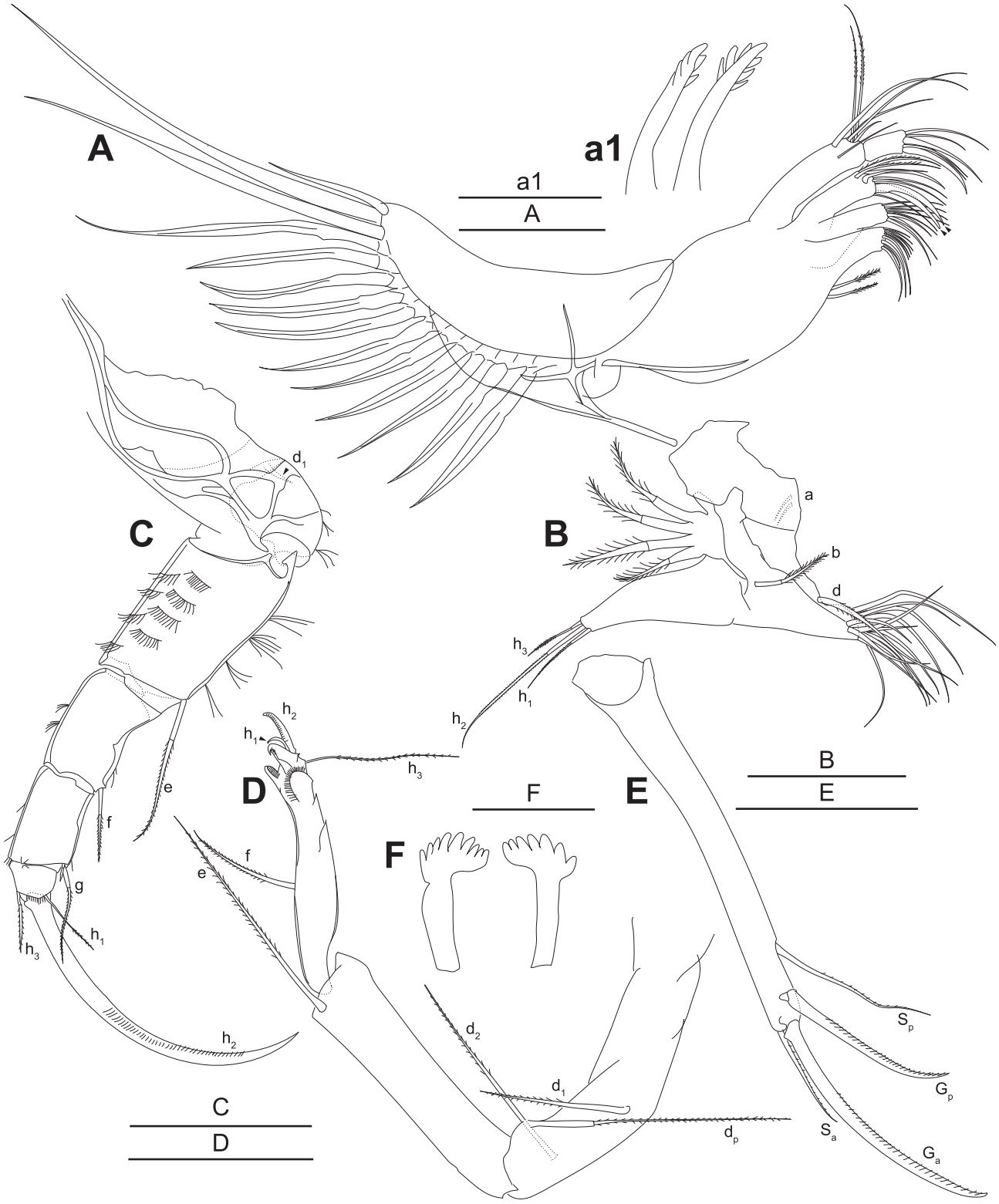

Fig. 6. *Heterocypris spadix* sp. nov., female, holotype (ICHUM-6128). **(A)** Mx (some rays lost during dissection; arrowheads, distal serrated spines). **(a1)** serrated spines on third endite of Mx. **(B–D)** L5–7 (setules of distal setae on L5 protopod omitted). **(E)** UR. **(F)** rake organ. Scale bars: **(A–E)** 0.1 mm, **(a1, F)** 0.05 mm.

formed by third and fourth podomeres. First podomere (protopod) with plumed setae $d_{1,2,p}$. Second (first endopodal) podomere with ventrodistal plumed seta e slightly shorter than podomeres 3–5. Third podomere with mid-ventral plumed seta f not reaching tip of L7. Fourth podomere with long plumed seta h_3, hook-like seta h_2, and tiny seta h_1.

UR (Fig. 6E) with UR-L/UR-W ratio ca. 11. L ratio of ramus, plumed seta S_a, claw G_a, claw G_p, and plumed seta S_p 7 : 2 : 4 : 3 : 3.

Rake organ (Fig. 6F) with stout rod and seven to nine blunt distal teeth.

Variation. We dissected three specimens and observed their appendages. As the rays on the vibratory plates are easily detached during dissection (Karanovic, 2012), the degree of variation in the ray numbers on Md, Mx, and L5 could not be determined; the numbers of rays observed on these appendages varied among specimens. The length of seta f on the fourth podomere of L6 varied among specimens; some extended beyond the tip of the fifth podomere whereas others did not.

Breeding and desiccation experiments. F_1 individuals (n = 20) from six P individuals hatched 1–19 days (average, 3.35 days) after spawning. Fourteen of these 20 F_1 individuals reached the adult stage and spawned 13–35 days (average, 20.2 days) after hatching. Two F_2 individuals isolated from a single egg mass hatched one day after spawning and themselves spawned 22–27 days (average, 24.5 days) after hatching. We found no males in our aquarium.

Four of the 12 individuals (33.3%) in the 1h-drying treatment were alive at 1 hour after and 1 day after rehydration. No living individuals were observed in the other treatments, with the survival rates thus being 0%.

Molecular analysis

The partial COI sequence (658 nt, encoding 219 amino acids; the INSD accession number LC557032) and the nearly complete 18S sequence (1762 nt; LC557033) were determined from one specimen (ICHUM-6135). For COI (489 nt in the aligned dataset), the K2P distances between our sequence and those from three *Heterocypris* species in the INSD (three sequences from *H. salina* from Egypt, one from *H. incongruens* from Turkey, and one from *Heterocypris* sp. from Italy) were 19.0–19.2%, 25.1%, and 25.9%, respectively. The sequences in the INSD most similar to our sequences, determined by BLAST searches (Altschul et al., 1990), were from *H. salina* (INSD accession number LC324690; identity score 84.07%, query cover 99%; Ali et al., 2018) for COI, and from *Heterocypris* sp. 3 China (INSD accession number KM403077.1; identity score 99.75%, query cover 100%; Kong et al., 2014) for 18S.

A 907-nt *Cardinium* 16S sequence (LC589665) was amplified and sequenced from specimen ICHUM-6135. The sequence in the INSD most similar to our sequence, determined by a BLAST search, was "*Candidatus* Cardinium sp. Hi1C" from *Heterocypris incongruens* (INSD accession number MH908934.1; identity score 99.52%, query cover 91%; Schön et al., 2018). Although Schön et al. (2018) also detected *Cardinium* in *H. salina*, no corresponding sequence is deposited in the INSD.

DISCUSSION

Heterocypris spadix sp. nov. differs from all congeners except *H. salina* in the following combination of features: (1) the carapace is pale yellowish in color, with dark-brown mottling; (2) LV overlaps RV along the entire free margin; (3) LV-L = 1.12 mm; (4) LV-H/LV-L and RV-H/RV-L = 0.62 and 0.60, respectively, with the former greater than the latter; (5) Ca-W/LV-L = 0.49; (6) the ventral margin of the carapace is concave; (7) the subanterior right margin of the carapace is weakly depressed in dorsal view; (8) tubercles are present on the anteroventral and posteroventral margins of RV; (9) claw G_2 is ca. 80% the length of claws $G_{1,3}$ on An2; (10) the fourth podomere of An2 undivided; (11) the second palpal podomere of Mx is rectangular rather than spatula-shaped, with L/W = ca. 2; (12) the L6 protopod has seta d_1 but lacks d_2; (13) seta e on L6 is long, reaching the middle of the fifth podomere; (14) UR-L/UR-W = ca. 11; and (15) the L ratio of the ramus, plumed seta S_a, claw G_a, claw G_p, and plumed seta S_p of UR is 7 : 2 : 4 : 3 : 3.

Heterocypris salina was originally described from England, UK (Brady, 1868), but has subsequently been reported from four zoogeographical regions spanning several continents (Meisch et al., 2019). Meisch (2000) described the morphology of the valves in detail for specimens from Germany, the nearest locality to the type locality (UK). Although *H. spadix* and *H. salina* are very similar, the former differs from the latter in the following features (also see Table 2): (1) the marginal infolds are less developed (e.g., RV-PMI/RV-L ≈ 3.7% in *H. spadix*, 6.8% in *H. salina*), (2) the tubercles on the anterior margin of the right valve are completely covered by the selvage and invisible in inner view (they are exposed and evident in inner view in *H. salina*), and (3) the calcified inner lamella on the ventral margin of the left and right valves is scarcely observable in inner view as the ventral margin of valves bends inward (evident in inner view in *H. salina*) (Meisch, 2000). At present, no COI DNA barcode sequences are available for European *H. salina*; the only sequences for this nominal species in the INSD were determined from specimens from Egypt by Ali et al. (2018). K2P distances for COI between *H. spadix* and the Egyptian *H. salina* were 19.0–19.2%, much higher than

Table 2. Relative lengths (%) of the anterior and posterior marginal infolds (AMI and PMI, respectively) to the left and right valve lengths (LV-L and RV-L, respectively) in *H. spadix* sp. nov. and *H. salina* (Brady). The measurements for *H. salina* are from Meisch (2000).

	H. spadix sp. nov. (ICHUM)											*H. salina*
	6136	6137	6138	6139	6140	6141	6142	6143	6144	6145	Range (Average)	
LV-AMI/LV-L	10.2	10.3	10.8	11.0	10.8	10.8	10.0	10.6	10.8	10.2	10.0–11.0 (10.6)	12.3
LV-PMI/LV-L	5.4	4.6	6.2	5.0	5.4	5.1	5.2	4.7	5.1	4.5	4.5–6.2 (5.1)	8.3
RV-AMI/RV-L	9.1	8.8	9.0	8.8	9.4	9.3	8.5	9.0	9.0	8.9	8.5–9.4 (9.0)	11.3
RV-PMI/RV-L	3.4	3.8	3.5	4.0	3.9	3.7	3.4	3.8	3.9	3.5	3.4–4.0 (3.7)	6.8

interspecific distances previously reported for other cypridoidean ostracods: 6.1% *p*-distance for *Bennelongia* De Deckker and McKenzie, 1981 (Martens et al., 2013); 4.0–6.1% K2P distance for *Physocypria* Vávra, 1897 (Karanovic, 2015).

Our sample comprised only females, and our breeding experiment showed that they can reproduce parthenogenetically for at least two generations. We obtained a 16S sequence from the bacterial endosymbiont *Cardinium* from one *H. spadix* individual. Schön and Martens (2019) reported *Cardinium* infections in females of several *Heterocypris* species with mixed and asexual reproduction, and speculated that the *Cardinium* infection may have affected the reproductive mode, as in many other arthropods (e.g., Ma and Schwander, 2017).

Our desiccation experiment showed that *H. spadix* has a low tolerance for drying; except for four individuals that survived 1 hour of desiccation, all individuals in the experiment died. This indicates that, under the condition at 25°C, a desiccation period of somewhere between 1 and 2 hours is lethal to *H. spadix*. Ostracod individuals attached to birds' feet or plumage are believed to survive long-distance transport (Meisch, 2000). However, our result suggests that such long-distance transport via birds may be less probable for *H. spadix*.

ACKNOWLEDGMENTS

We thank the staff of the Manko Waterbird & Wetland Center for the use of facilities during sampling; Akira Tsukagoshi for literature; Takeo Horiguchi for comments on results; Chizue Hiruta for help in rearing ostracods; Yuki Oya for help in molecular analyses; and Matthew H. Dick for reviewing the manuscript and editing the English. This study was supported in part by a KAKENHI grant (JP16K18597) from the Japan Society for the Promotion of Science (JSPS) to KK.

COMPETING INTERESTS

We declare no competing interests.

AUTHOR CONTRIBUTIONS

MM conceived and designed the study, made morphological observations, and conducted the molecular analysis and breeding experiments. KK collected and reared the ostracods. MM, HT, and KK all contributed to writing the manuscript, and have read and approved the final draft.

REFERENCES

Ali FS, Yousef EA, Hegab MH, Khalifa N (2018) Morphological redescription and molecular characterization of *Heterocypris salina* (Brady, 1868), a new recorded ostracod species in Egypt. Egypt J Aquat Biol Fish 22: 37–54

Altschul SF, Gish W, Miller W, Myers EW, Lipman DJ (1990) Basic local alignment search tool. J Mol Biol 215: 403–410

Baird W (1845) Arrangement of the British Entomostraca, with a list of species, particularly noticing those which have as yet been discovered within the bounds of the Club. Hist Berwickshire Nat Club 2: 145–158

Brady GS (1868) A monograph of the recent British Ostracoda. Trans Linn Soc Lond 26: 353–495 + pls 23–41

Broodbakker NW (1988) Ecology and distribution of groundwater Crustacea and freshwater Ostracoda in SW Honshu and the Nansei Islands, Japan. Versl Tech Gegevens Inst Taxon Zool (Zool Mus) Univ Amst 53: 1–21

Broodbakker NW, Danielopol DL (1982) The chaetotaxy of Cypridacea (Crustacea, Ostracoda) limbs: proposals for a descriptive model. Bijdr Dierk 52: 103–120

Claus C (1892) Beiträge zur Kenntnis der Süsswasser-Ostracoden, I. Ueber den Körper- und Gliedmassenbau der Cypriden nebst Bemerkungen über einzelne innere Organe derelben. Arb Zool Inst Univ Wien Zool Stat Triest 10: 147–216

Folmer O, Black M, Hoeh W, Lutz R, Vrijenhoek R (1994) DNA primers for amplification of mitochondrial cytochrome *c* oxidase subunit I from diverse metazoan invertebrates. Mol Mar Biol Biotechnol 3: 294–299

Gotoh T, Noda H, Ito S (2007) *Cardinium* symbionts cause cytoplasmic incompatibility in spider mites. Heredity 98: 13–20

Hiruta S, Smith RJ (2001) Living freshwater and shallow marine Ostracoda in eastern Hokkaido, Japan. In "Guidebook of Excursions of the 14th International Symposium on Ostracoda" Ed by N Ikeya, Organizing Committee of ISO 2001, Shizuoka, pp 107–125

Karanovic I (2012) Recent Freshwater Ostracods of the World. Springer, Berlin

Karanovic I (2015) Barcoding of ancient lake ostracods (Crustacea) reveals cryptic speciation with extremely low distances. PLOS ONE 10: e0121133

Kimura M (1980) A simple method for estimating evolutionary rates of base substitutions through comparative studies of nucleotide sequences. J Mol Evol 16: 111–120

Kong Q, Karanovic I, Yu N (2014) Phylogeny of the genus *Chrissia* (Ostracoda: Cyprididae) with description of a new species from China. J Crustacean Biol 34: 782–794

Kubanç N, Taşçi T, Kubanç C, Özuluğ O, Eldem V (2017) A quick and efficient method for DNA isolation from freshwater ostracods. Genet Aquat Org 1: 1–7

Kumar S, Stecher G, Tamura K (2016) MEGA7: Molecular evolutionary genetics analysis version 7.0 for bigger datasets. Mol Biol Evol 33: 1870–1874

Ma WJ, Schwander T (2017) Patterns and mechanisms in instances of endosymbiont-induced parthenogenesis. J Evol Biol 30: 868–888

Maraun M, Erdmann G, Schulz G, Norton RA, Scheu S, Domes K (2009) Multiple convergent evolution of arboreal life in oribatid mites indicates the primacy of ecology. Proc R Soc B 276: 3219–3227

Martens K (1987) Homology and functional morphology of the sexual dimorphism in the antenna of *Sclerocypris* Sars, 1924 (Crustacea, Ostracoda, Megalocypridinae). Bijdr Dierk 57: 183–190

Martens K, Halse S, Schön I (2013) On the *Bennelongia barangaroo* lineage (Crustacea, Ostracoda) in Western Australia, with the description of seven new species. Eur J Taxon 66: 1–59

Martens K, Yavuzatmaca M, Higuti J (2019) On a new species of the genus *Cyprinotus* (Crustacea, Ostracoda) from a temporary wetland in New Caledonia (Pacific Ocean), with a reappraisal of the genus. Eur J Taxon 566: 1–22

Meisch C (2000) Freshwater Ostracoda of Western and Central Europe. Spektrum Akademischer Verlag, Berlin

Meisch C (2007) On the origin of the putative furca of the Ostracoda (Crustacea). Hydrobiologia 585: 181–200

Meisch C, Smith RJ, Martens K (2019) A subjective global checklist of the extant non-marine Ostracoda (Crustacea). Eur J Taxon 492: 1–135

Nakayama T, Watanabe S, Mitsui K, Uchida H, Inoue I (1996) The phylogenetic relationship between the Chlamydomonadales and Chlorococcales inferred from 18SrDNA sequence data. Phycol Res 44: 47–55

Okubo I (1972) Freshwater Ostracoda from Japan, IV. *Heterocypris incongruens* (Ramdohr, 1808). Res Bull Shujitsu Jr Coll, Okayama 1: 73–84

Okubo I (1973) *Heterocypris takedai* sp. nov. (Ostracoda, Cyprididae) from Japan. Annot Zool Jpn 46: 85–89
Okubo I (1975) Studies on Ostracoda in fishponds I. Two species in fishponds of the Chiba Prefectural Freshwater Fisheries Experimental Station. Bull Jpn Soc Sci Fish 41: 155–165
Okubo I (2004) Freshwater Ostracoda from Japan. Mikado Printing Office, Okayama (in Japanese)
Okubo I, Ida K (1989) Freshwater Ostracoda from Gunma Prefecture, Japan. Bull Biogeogr Soc Jpn 44: 105–107 (in Japanese with English abstract)
Okubo I, Terauchi M (1992) Freshwater Ostracoda from the Southwestern Islands of Japan. Proc Jpn Soc Syst Zool 46: 101–108
Puitika T, Kasahara Y, Miyoshi N, Sato Y, Shimano S (2007) A taxon-specific oligonucleotide primer set for PCR-based detection of soil ciliate. Microbes Environ 22: 78–81
Rasband WS (2020) ImageJ. Available at: https://imagej.nih.gov/ij/
Rossi V, Gandolfi A, Baraldi F, Bellavere C, Menozzi P (2007) Phylogenetic relationships of coexisting *Heterocypris* (Crustacea, Ostracoda) lineages with different reproductive modes from Lampedusa Island (Italy). Mol Phylogenet Evol 44: 1273–1283
Savatenalinton S (2020) Description of a new species of *Heterocypris* Claus, 1892 (Crustacea: Ostracoda: Cyprididae) from Thailand. Raffles Bull Zool 68: 70–79
Schön I, Martens K (2019) Are *Cardinium* infections causing asexuality in non-marine ostracods?. Hydrobiologia 847: 1651–1661
Schön I, Kamiya T, Van den Berghe T, Van den Broecke L, Martens K (2018) Novel *Cardinium* strains in non-marine ostracod (Crustacea) hosts from natural populations. Mol Phylogenet Evol 130: 406–415
Smith RJ, Chang CY (2020) Taxonomic assessments of some Cyprinotinae Bronstein, 1947 species (Crustacea: Ostracoda) from Japanese and Korean rice fields, including (re-) descriptions of six species and a review of the type species of the subfamily. Zootaxa 4795: 1–69
Smith RJ, Kamiya T (2006) Six new species of fresh and brackish water ostracods (Crustacea) from Yakushima, Southern Japan. Hydrobiologia 559: 331–355
Smith RJ, Janz H, Okubo I (2011) Recent Cyprididae and Ilyocyprididae (Crustacea: Ostracoda) from Lake Biwa, Japan, including a summary of the lake's ostracod fauna. Zootaxa 2874: 1–37
Tabuki R, Hashimoto M (2012) Freshwater ostracode fauna from 'Taimo' field of Oyama, Ginowan City in the Middle Part of Okinawa Island, Japan. Bull Fac Educ Univ Ryukyus 80: 235–241 (in Japanese with English abstract)
Tanaka H, Kotorii H, Yokozawa K, Wakabayashi F, Kimoto K, Sano K (2015) Distribution and occurrence of freshwater Ostracoda (Crustacea) from southwest region of Mt. Fuji. Taxa 38: 26–41 (in Japanese with English abstract)
Thompson JD, Higgins DG, Gibson TJ (1994) CLUSTAL W: improving the sensitivity of progressive multiple sequence alignment through sequence weighting, position-specific gap penalties and weight matrix choice. Nucleic Acids Res 22: 4673–4680
Yamada S, Keyser D (2010) Calcification of the marginal infold in podocopid ostracods. Hydrobiologia 638: 213–222
Zchori-Fein E, Perlman SJ (2004) Distribution of the bacterial symbiont *Cardinium* in arthropods. Mol Ecol 13: 2009–2016

(Received July 30, 2020 / Accepted December 23, 2020 / Published online February 25, 2021)